

Review

MXene Film Prepared by Vacuum-Assisted Filtration: Properties and Applications

Jingfeng Wang * , Jiabei He , Dongxiao Kan, Kaiyun Chen, Mengshan Song and Wangtu Huo *

Northwest Institute for Nonferrous Metal Research, Xi'an 710016, China; hjb6260872008@hotmail.com (J.H.); dxkan1202@126.com (D.K.); chenkaiyun309@gmail.com (K.C.); febrisong2015@163.com (M.S.)

* Correspondence: wangjingfeng@163.com (J.W.); huowt@c-nin.com (W.H.)

Abstract: MXene ($Ti_3C_2T_x$) film prepared by vacuum-assisted filtration (V-MXene film) is the most common 2D MXene macroscopic assembly with ultra-high electrical conductivity, tunable interlayer space, diverse surface chemical properties, favorable mechanical properties and so on, showing great commercial value in the fields of energy storage, electromagnetic interference shielding and actuators and so on. This paper focuses on the preparation, properties and applications of V-MXene film, objectively reviews and evaluates the important research progress of V-MXene film in recent years and analyzes the main problems at present. In addition, the development direction and trend of V-MXene film in the future are prospected from the aspects of preparation, property control and application fields, which provide guidance and inspiration for the further development of functional MXene-based films and make contributions to the progress of MXene technology.

Keywords: MXene film; vacuum-assisted filtration; high conductivity; energy storage; electromagnetic interference shielding



Citation: Wang, J.; He, J.; Kan, D.; Chen, K.; Song, M.; Huo, W. MXene Film Prepared by Vacuum-Assisted Filtration: Properties and Applications. *Crystals* **2022**, *12*, 1034. <https://doi.org/10.3390/cryst12081034>

Academic Editor: Fei Gao

Received: 29 June 2022

Accepted: 23 July 2022

Published: 26 July 2022

Publisher's Note: MDPI stays neutral with regard to jurisdictional claims in published maps and institutional affiliations.



Copyright: © 2022 by the authors. Licensee MDPI, Basel, Switzerland. This article is an open access article distributed under the terms and conditions of the Creative Commons Attribution (CC BY) license (<https://creativecommons.org/licenses/by/4.0/>).

1. Introduction

After 11 years of development, MXenes (the general formula is $M_{n+1}X_nT_x$, where M is transition metal element, X is C or N, T_x represents terminal surface groups such as $-OH/-F/-O$ and $n = 1-4$) have been developed into a huge family of materials. There are currently more than 30 stoichiometric MXene [1], and more than 100 theoretically predicted MXenes [2]. $Ti_3C_2T_x$ is a typical representative of MXene, and it is also one of the earliest prepared and most studied MXene. $Ti_3C_2T_x$ has the best comprehensive properties, with ultra-high electrical conductivity [3,4], hydrophilicity [5–7], solution processability [8,9], outstanding mechanical properties [10] and oxidation resistance, etc. [3], which enable MXene ($Ti_3C_2T_x$) to be applied in numerous fields [11–13].

The application of MXene needs to be based on a certain form of macroscopic assembly. At present, common MXene macroscopic assemblies mainly include MXene fibers [14,15], MXene films and three-dimensional MXene frameworks [16–20]. Among them, MXene films are the most common and most potential MXene macroscopic assembly, because MXene has a series of promising properties such as good mechanical property, hydrophilicity and processability [21], which is suitable for the preparation of film materials [22]. Additionally, MXene films are also expected to be fabricated on a large scale.

In recent years, MXene has been assembled into MXene films by various methods, including vacuum-assisted filtration (VAF), blade-coating [10], drop-casting [23], spin-coating [24], spray-coating [25], inkjet-printing [26], layer-by-layer assembly [27], natural sedimentation [28], roll-to-roll [29] and deposition technology [30]. Since the operation is simple and complex equipment is not required [31], VAF is the most commonly used and widely studied method for preparing MXene films at present despite the fact that MXene films with better performance in some aspects (such as electrical conductivity and mechanical properties) can be prepared by other methods such as blade-coating and drop-casting.

This review briefly introduces the preparation methods of MXene ($\text{Ti}_3\text{C}_2\text{T}_x$), the preparation process of MXene films via VAF (named V-MXene films), the properties of V-MXene films, and summarizes the important research progress of V-MXene film materials and their applications in different fields. Finally, the existing problems, future development direction and trend of V-MXene films are prospected.

2. Preparation of MXene

MXene is mainly prepared by selectively etching element A (such as Al) in the MAX (mainly Ti_3AlC_2) phase of its precursor. The in situ HF generation method (Figure 1a) is the most common and effective method for preparing single-layer MXene nanosheets at present. Its principle is to generate hydrofluoric acid (HF) in situ on the surface of the MAX phase through the mixed solution of HCl and LIF to realize the etching of Al. This method has the advantages of mild reaction, safety and effectiveness, less damage to MXene lattice, and can avoid the use of additional intercalators. More importantly, it can realize large-scale preparation without losing MXene performance [32]. Moreover, combined with cellulose-assisted exfoliation, the preparation of single-layer large-size MXene nanosheets ($4\ \mu\text{m}$) can be achieved only by manual shaking [33]. Other methods such as ammonium hydrogen fluoride (NH_4HF_2) etching [34], fluoride-free etching [35–38], and water-free etching [39] can also be used to synthesize MXene. Recently, Li et al. [40,41] synthesized MXene with a Cl surface functional group ($\text{Ti}_3\text{C}_2\text{Cl}_2$) at high temperature by using the molten chloride salt of Lewis acid (such as ZnCl_2) (Figure 1b). The molten salt method has extraordinarily good universality and can realize the etching of a variety of MXenes (such as Ti_2CT_x , Nb_2CT_x and $\text{Ti}_3\text{C}_2\text{T}_x$). Through the intercalation of intercalants such as tetrabutylammonium hydroxide (TBAOH), the exfoliation of multi-layer MXene can be achieved [42]. Moreover, MXene with good dispersion in organic solvents can be prepared through tuned microenvironment method [43]. In addition to Ti_3AlC_2 , $\text{Ti}_3\text{C}_2\text{T}_x$ MXene [44] can also be obtained by selective etching of Si in Ti_3SiC_2 , and its oxidation resistance is more favorable. MXene ($\text{Ti}_3\text{C}_2\text{T}_x$ and Ti_2CT_x) can also be prepared by one pot method using titanium powder, aluminum powder and carbon powder as raw materials (without direct use of MAX precursor). This method is not only safe and easy to operate, but also does not need inert gas during preparation [45]. The properties of MXene prepared by different methods are different; thus, it is necessary to select the appropriate method according to the desired purpose.

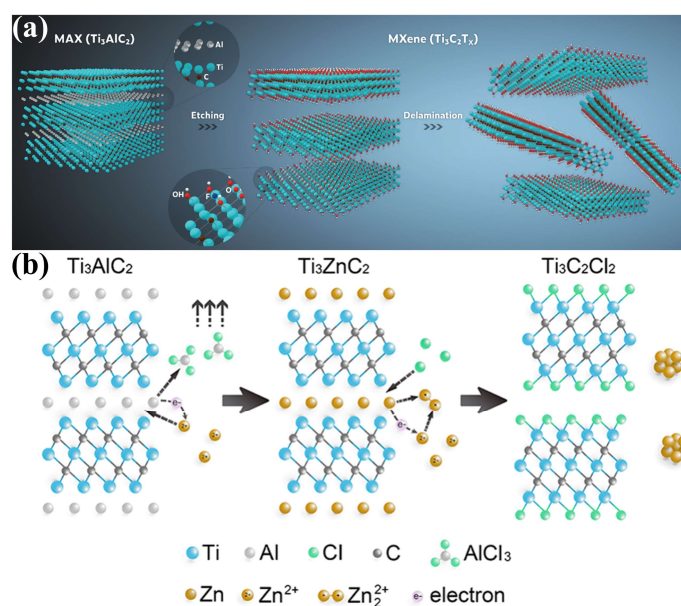


Figure 1. (a) Preparation of MXene by in situ generation HF method. Reproduced from [46], with the permission of the Royal Society of Chemistry. (b) Preparation of MXene by the molten salt method. Reproduced from [40], with the permission of the American Chemical Society.

3. The Preparation Process of V-MXene Film and Its Properties

The preparation process of V-MXene film is as follows: filter the MXene dispersion on the porous filter membrane, and the MXene nanosheets in the dispersion will quickly cover the pore surface of the filter membrane, and gel at the interface in the way of face-to-face dense arrangement. The capillary compression force perpendicular to the MXene nanosheets generated in the subsequent evaporation of water will make the MXene sheets arrange extremely closely. After filtration and drying, the V-MXene film on the surface of the filter membrane can be peeled off. As MXene is a high barrier two-dimensional material with high aspect ratio, water molecules can only flow along the edge of MXene nanosheet during the preparation of V-MXene film, which greatly increases the transportation path and difficulty of water molecules. Therefore, the preparation of V-MXene film takes a lot of time. To enhance the preparation efficiency, our group [47] used electrolyte ions to induce MXene colloidal dispersion to transform into a micro gel with three-dimensional structure (Figure 2), which shortened the preparation time from a few hours to more than 10 s, and V-MXene films still exhibit outstanding electrical conductivity and mechanical properties.

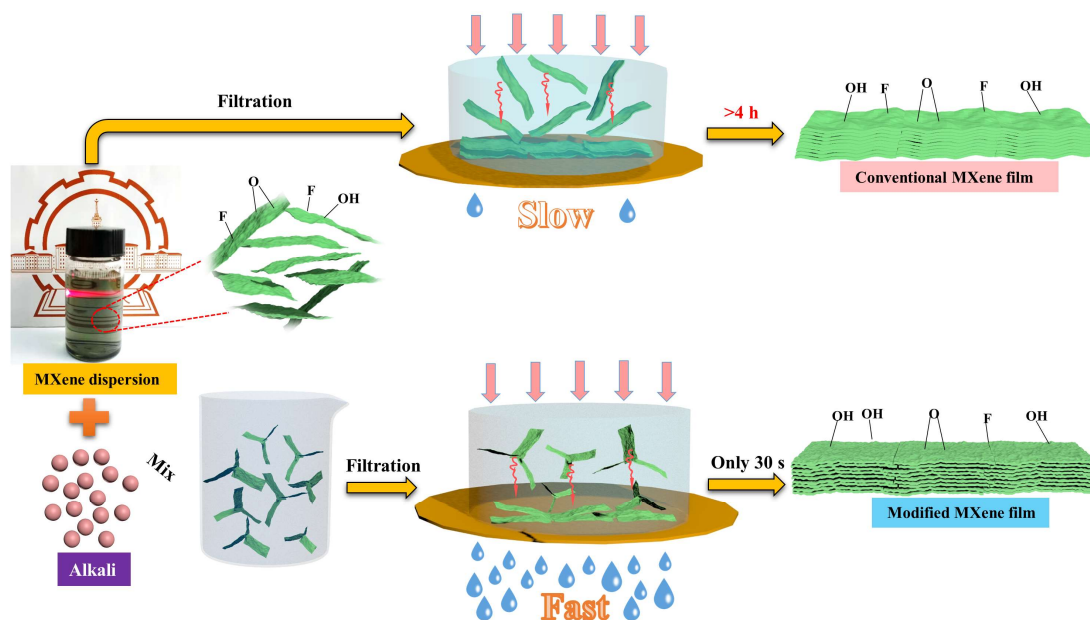


Figure 2. MXene film prepared by electrolyte-induced flocculation combined with vacuum-assisted filtration. Reproduced from [47], with the permission of the Engineered Science Publisher.

Owing to the dense arrangement of MXene nanosheets, V-MXene films have a variety of perfect properties, such as ultra-high electrical conductivity, favorable mechanical properties, and outstanding oxidation resistance. The following focuses on the properties of V-MXene films.

3.1. Electrical Conductivity

Owing to the high electron density of states near the Fermi level $[N(E_f)]$, MXene is metallic in nature; as a result, MXene nanosheets have low in-plane resistance, which is affected by the etching process, the size and defects of the nanosheets, contents of surface functional groups, MAX phase structure, and other factors. By optimizing the preparation process, MXene nanosheets can have larger size, fewer defects and oxidation (Figure 3) under the condition of good exfoliation, so as to expand the electrical conductivity of MXene nanosheets [48]. MXene without any functional groups is metallic [49], while the presence of surface functional groups makes MXene a narrow-band semiconductor. By removing surface functional groups, the electrical conductivity of MXene can be enhanced [50]. Furthermore, by optimizing the structure of MAX phase used in the preparation of MXene,

the researchers [3] synthesized high-quality MXene nanosheets. The electrical conductivity of the corresponding V-MXene film is as high as $20,000 \text{ S cm}^{-1}$, which is the highest electrical conductivity of MXene film at present.

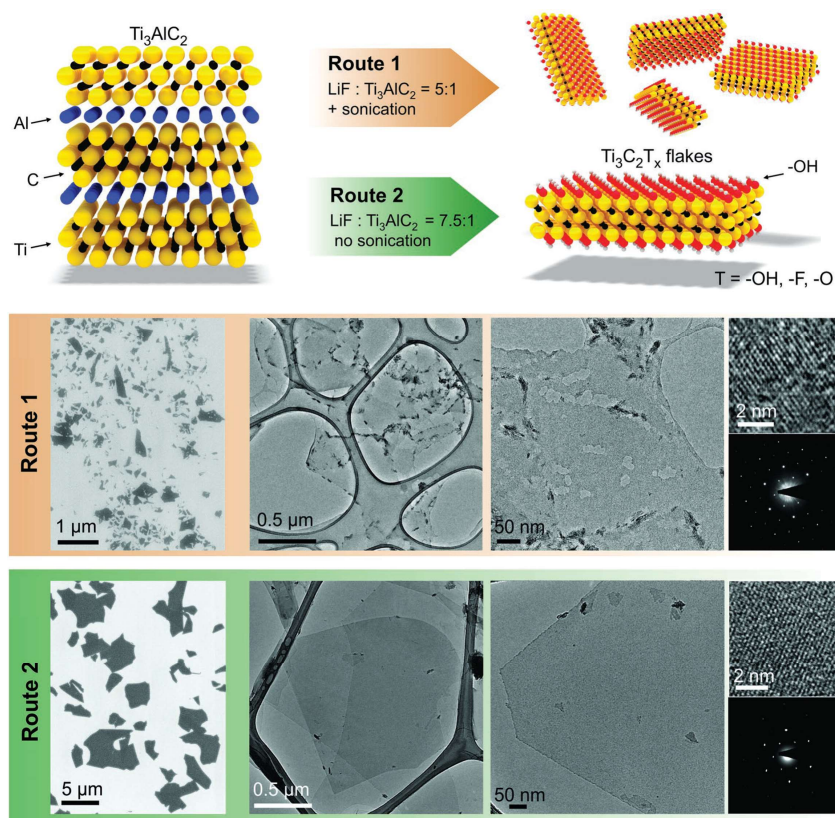


Figure 3. Preparation and characterization of MXene flakes produced by various routes. Reproduced from [48], with the permission of Wiley-VCH.

For V-MXene films, the electrical conductivity is also closely related to the interface contact resistance between MXene sheets (such as the resistance perpendicular to the base plane of MXene nanosheets, i.e., out-of-plane resistance), and its value is affected by the interaction between MXene nanosheets, the degree of orientation of MXene nanosheets and the compactness of V-MXene films. It should be noted that the influence law of these factors on the electrical conductivity of MXene films prepared by other solution processing methods (such as blade-coating and drop-casting) is similar. As a result of the contact resistance at the interface, the electrical conductivity of the single-layer MXene nanosheet and the corresponding V-MXene film differs by nearly an order of magnitude [48]. However, this difference is actually quite small. In graphite (stacked two-dimensional graphene nanosheets), the resistance difference between vertical and parallel to the base plane of graphene nanosheets can reach three orders of magnitude [51]. Through adjusting the mechanical load (such as compression or stretching) perpendicular to the base plane, the difference between in-plane resistance and out-of-plane resistance can be controlled well. When MXene sheets are pressed with each other, they can be made equal [52]. Moreover, the removal of intercalant (such as metal ions [53] or water molecules [54]) between MXene nanosheets, or appropriate cross-linking of MXene nanosheets [55], is conducive to increasing the interlayer interaction of MXene nanosheets, improving the arrangement of nanosheets, enhancing the compactness of V-MXene films, and thus elevating the electrical conductivity of V-MXene films.

3.2. Mechanical Property

MXene has favorable mechanical properties. Molecular dynamics simulation shows that the Young's modulus of MXene is 502 GPa [56]. On account of the presence of surface groups and defects, the actual measured value is 333 GPa [57]. For pure V-MXene films, there is no primary bonding between MXene nanosheets; as a consequence, inter-layer sliding is the main deformation mechanism in the process of tensile loading in MXene film [58,59]. The larger the size of the MXene nanosheet, the higher the break strain, tensile strength and stiffness of the V-MXene film. The result is due to the longer sliding distance of the MXene nanosheet before the break of the V-MXene film [10], less sheet-to-sheet contact defect between the nanosheets [58] and the longer shear stress transfer length [58], respectively. Density functional theory [60] shows that the existence of surface functional groups of MXene can promote the "bonding" between MXene nanosheets, and can provide sliding resistance in the form of mechanical interlocking to resist the sliding of MXene nanosheets when the film is subjected to external forces. Additionally, the mechanical properties of V-MXene films also depend on the compactness of the films, the interaction between MXene nanosheets and the degree of orientation of MXene nanosheets. By removing intercalant (such as metal ions [53]) between MXene nanosheets, the interlayer interaction and the compactness of the film can be increased, thereby improving the mechanical properties of V-MXene films. The tensile strength of thicker V-MXene films is generally lower [10], which is also on account of the weaker interlayer interaction and lower compactness. For the sake of further enhancing the mechanical properties of V-MXene films, materials that show stronger binding with MXene are often introduced into the MXene system to prepare V-MXene composite film, including polymers [31,61,62], cellulose nanofibers [63], pyrrole [64], nanomaterials (such as graphene oxide [65] and carbon nanotubes [66]) and so on. The interactions between these materials and MXene include hydrogen bond [31], ionic bond [67], covalent bond [55] and synergistic interfacial interaction [55,65,67]. Synergistic interfacial interaction is an effective means to strengthen the mechanical properties of V-MXene films. The interaction between MXene nanosheets, the degree of orientation of MXene nanosheets and the compactness of V-MXene films can be raised through the synergism of hydrogen bond and ion bond [67] (Figure 4). The tensile strength, toughness and Young's modulus of the obtained V-MXene films are 436 MPa, 8.39 MJ/cm³ and 14 GPa, respectively. By further induction of the densification and void removal of V-MXene film through sequential bridging of hydrogen bond and covalent bond [55], a highly dense V-MXene film can be obtained, and its tensile strength can reach 583 MPa, which is the highest value of MXene film at present. Additionally, the toughness and Young's modulus are 15.9 MJ/cm³ and 27.8 GPa, respectively.

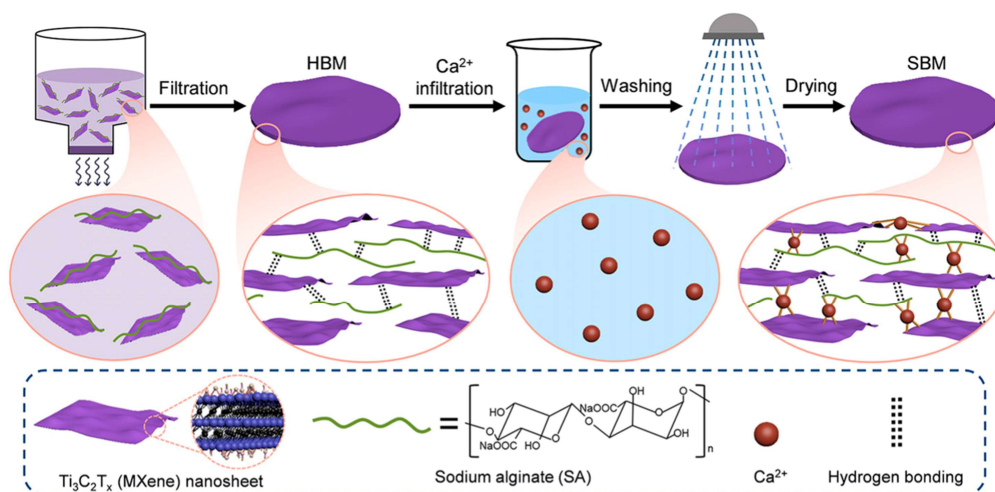


Figure 4. Schematic illustration of preparation of V-MXene film through sequential bridging of hydrogen and ionic bonding. Reproduced from [67], with the permission of National Academy of Science.

3.3. Oxidation Stability

MXene is easily oxidized in aqueous solution and oxygen-containing environment [68]. After the MXene dispersion is assembled into V-MXene film, its oxidation resistance is greatly strengthened. However, because of the presence of water molecules between layers of V-MXene films [69] and moisture and oxygen at room temperature, V-MXene films will still be oxidized [70]. For the purpose of fundamentally promoting the oxidation resistance of V-MXene films, Mathis et al. [3] optimized the synthesis of MXene nanosheets and obtained V-MXene films that can withstand a high temperature of up to 450 °C (Figure 5). Another way to enhance the oxidation resistance of V-MXene film is to create conditions that are not beneficial to the oxidation of V-MXene film, including optimizing the storage conditions (such as lower temperature and humidity [70]) or isolating the contact between H₂O/O₂ and MXene nanosheet. The contact between H₂O/O₂ and MXene nanosheets can be isolated by improving the interaction between MXene nanosheets, the compactness of V-MXene films [53], introducing polymer [71] or high barrier materials [72] (such as graphene oxide, which blocks oxygen), and the above-mentioned synergy [55,67]. Specifically, bridging and covering MXene nanosheets with metal ions (such as Ca²⁺) and polymers can greatly increase the oxidation stability of V-MXene films [67], since ionic bonding can reduce the interplanar spacing of the nanosheets and prevent the insertion of H₂O/O₂, while the addition of polymers can prevent MXene nanosheets from contacting H₂O/O₂. The covalent bridging of MXene nanosheets and removal of the voids in V-MXene films with covalent crosslinking agents (such as borate ions) and polymers can further raise the compactness of V-MXene films and drop the overall structural defects [55]; therefore, V-MXene films with better oxidation resistance can be obtained.

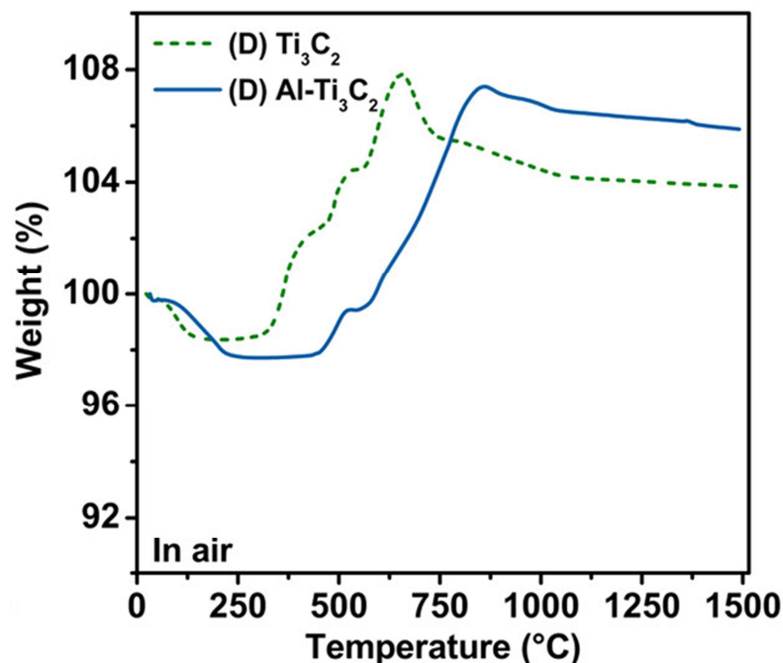


Figure 5. Thermogravimetric analysis of V-MXene films with high oxidation resistance (solid lines). Reproduced from [3], with the permission of the American Chemical Society.

3.4. Wetting Property

MXene demonstrates remarkable hydrophilicity, which is retained by V-MXene films. For some special applications, it is necessary to control the hydrophilicity/hydrophobicity of V-MXene films purposefully. For example, in water purification applications [73,74], the higher the hydrophilicity of V-MXene film, the more advantageous to the adsorption and reduction of heavy metal ions. The surface hydroxylation of Ti-O_x terminal groups on the surface of MXene into Ti-(OH)_x by HCl treatment can enhance the hydrophilicity

of V-MXene films [74]. What is more, our previous research shows that [47] replacing the hydrophobic $-F$ on the surface of MXene with $-OH$ by using strong base can also improve the hydrophilicity of V-MXene films. On the other hand, V-MXene film will adsorb moisture and gas in the environment due to the hydrophilicity, which is detrimental to its application in sensors and other fields. Moreover, the poor hydration stability of V-MXene film will lead to swelling, affecting the mechanical and electrical properties of the film material [59], so it is necessary to prepare hydrophobic V-MXene film. Surface modification is a common method to prepare hydrophobic V-MXene films. By modifying V-MXene films with octadecyl isocyanate [75], porphyrin [76] and fluorosilane [77,78], a range of hydrophobic V-MXene films have been obtained with contact angles ranging from 102° to 143.9° . The hydrophobicity of V-MXene films can also be strengthened by removing the hydrophilic functional groups of MXene by calcination. Fan et al. [79] prepared porous V-MXene films by template-sacrificing strategy. After calcination at 200 and 300°C , the contact angles of porous V-MXene films were 81° and 101° , respectively. The storage time and drying process of V-MXene film will also affect the wettability. With the extension of storage time, the naturally dried V-MXene film (MXene-N) will be more hydrophobic (Figure 6a), while the oven-dried V-MXene film (MXene-O) will be more hydrophilic (Figure 6b), which may be related to the pollution and oxidation of V-MXene film [80].

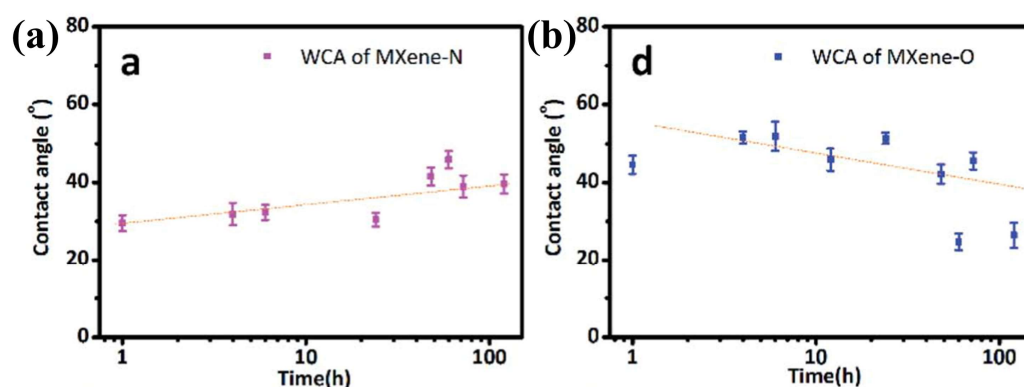


Figure 6. Water contact angle of MXene-N (a) and MXene-O (b) over storing time. Reproduced from [80], with the permission of the Royal Society of Chemistry.

3.5. Others

In the filtration process, MXene nanosheets are arranged in the manner of face-to-face; as a result, the V-MXene film structure is quite dense, which is extremely unfavorable to the application of V-MXene films in energy storage and other fields. For this reason, V-MXene films with pore structure have been prepared through hard template method [79], foaming method [81,82] and synthesis of porous MXene nanosheets [83]. For example, Ren et al. [83] obtained porous MXene nanosheets through chemical etching, and then assembled them to obtain porous V-MXene films (Figure 7a).

On the other hand, when V-MXene films are prepared, the size will be limited owing to the restriction of filtration equipment, and it is difficult to build this V-MXene film into a more widely used three-dimensional complex structure. To expand the size of V-MXene film and better construct the three-dimensional complex structure, our group [84] proposed a time-sensitive welding concept of V-MXene film (Figure 7b), and realized the construction of large-size V-MXene film and three-dimensional complex structure based on V-MXene film with water as solder.

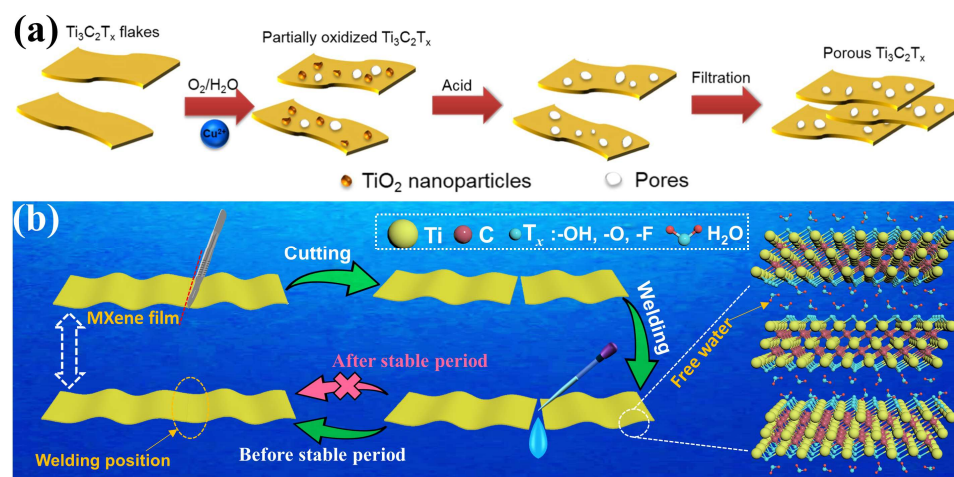


Figure 7. (a) Schematic illustration of preparation of porous MXene flakes by chemical etching. Reproduced from [83], with the permission of Wiley-VCH. (b) Schematic diagram of the welding process of MXene film. Reproduced from [84], with the permission of Elsevier.

4. Applications of V-MXene Film

V-MXene films have remarkable mechanical properties, ultra-high electrical conductivity, abundant terminal functional groups, outstanding hydrophilicity and other eminent characteristics. Therefore, at present, V-MXene films show great application potential in the fields of electrochemical energy storage (such as supercapacitors and batteries) and electromagnetic interference (EMI) shielding. Moreover, more applications of V-MXene films are also being developed, such as actuators, gas separation, photothermal conversion, infrared stealth and other fields.

4.1. Energy Storage

MXene has the advantages of two-dimensional layered structure, metallic conductivity, small band gap and hydrophilic functional surface [85]; accordingly, it has attracted great attention in the field of energy storage. Compared with other conventional electrode materials and structures, MXene film materials (such as V-MXene film) show great advantages in flexibility, tailorability and functionality, which makes them suitable for flexible, portable and highly integrated energy storage systems [22], such as supercapacitors and batteries. The favorable mechanical properties, high electrical conductivity and outstanding specific capacitance of V-MXene film are significantly in favor of its application in the field of supercapacitors. However, the nanosheets of pure V-MXene film will be stacked again; consequently, the accessibility to electrolyte ions is poor, which is harmful for the full utilization of the surface of MXene. For increasing the accessibility of MXene to electrolyte ions and to further strengthen the electrochemical performance of V-MXene films, many methods have been developed, such as interlayer regulation [86], surface modification [87], pore engineering [79,88], composite with other materials [89] and the above-mentioned synergy [90]. Furthermore, the traditional V-MXene film is always parallel to the current collector; consequently, the ion transport path is long and the rate capability is poor. The thicker the V-MXene film, the worse the electrochemical performance. Our group [84] prepared vertically aligned compact MXene electrodes based on V-MXene film with electrode performance almost independent of thickness through welding technology (Figure 8). As a result of the great reduction of ion transport path, the electrochemical performance of MXene electrodes has been significantly improved, with a scan rate of 2000 mV s^{-1} and a thickness of $105 \text{ }\mu\text{m}$, the volumetric capacitance of the electrode can still reach $\sim 225 \text{ F cm}^{-3}$.

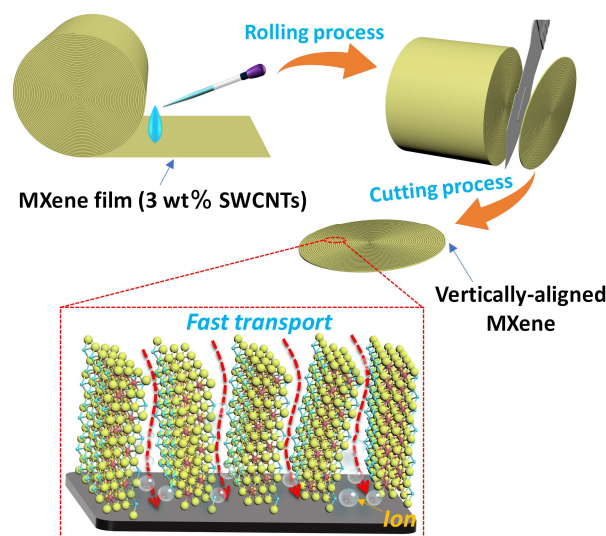


Figure 8. Schematic illustration of the preparation process of vertically aligned compact MXene electrode. Reproduced from [84], with the permission of the Elsevier.

Great progress has also been made in the application of V-MXene films in batteries (such as lithium ion batteries and sodium ion batteries). However, the re-stacking of MXene nanosheets is also pernicious to electrolyte penetration and ion transport. Its performance can be enhanced by means of nanochannel design [83,91], introduction of interlayer spacer [92] and surface modification [93]. For example, Chen et al. [94] obtained MXene/PEDOT hybrid films with pleasurable lithium ion storage performance by in situ polymerization of 3,4-ethylenedioxythiophene (EDOT) on the surface of MXene. The capacity of hybrid films increased from 195 mAh g^{-1} of pure MXene to 255 mAh g^{-1} . The enhancement of capacity may be the synergistic effect of the rapid diffusion of electrolyte and the surface redox process between PEDOT and MXene layers.

4.2. Electromagnetic Interference (EMI) Shielding

V-MXene film has become a candidate material with ideal EMI shielding effectiveness thanks to its ultra-high electrical conductivity. The electrical conductivity of V-MXene film is two orders of magnitude lower than that of pure metal. However, when the thickness is the same, the EMI shielding effectiveness of V-MXene film is almost close to that of pure metal film, since the layered structure also plays an important role. The research on the first application of V-MXene film to EMI shielding began in 2016 [95]. Thanks to the ultra-high electrical conductivity (4600 S cm^{-1}) and layered structure, when the thickness of V-MXene film is only $45 \text{ }\mu\text{m}$, its EMI shielding effectiveness can reach 92 dB, which is better than almost all the current electromagnetic shielding materials prepared by synthesis. Perfect EMI shielding performance mainly comes from the electromagnetic wave reflection caused by the favorable electrical conductivity of V-MXene film and the multiple internal reflection of electromagnetic wave between MXene nanosheets. Pure V-MXene films have poor mechanical properties when used as electromagnetic shielding materials. By removing the intercalant [53], using metal ion to crosslink MXene nanosheets [96], preparing MXene composite film [63,97] and structural design of V-MXene films (such as sandwich structure) [98], V-MXene films with enhanced mechanical properties and exceptional EMI shielding performance can be obtained. For example, in an effort to further expand the application of V-MXene film in the field of EMI shielding, Luo et al. [97] combined large deformation natural rubber with MXene to build MXene/natural rubber composite film. When the MXene volume fraction is only 6.71%, the EMI shielding effectiveness can reach 53.6 dB. V-MXene films mainly shield electromagnetic waves through reflection. With the purpose of enriching the electromagnetic wave loss mechanism, Liang et al. [99]

developed a flexible, conductive and magnetic “brick mortar” layered film with a variety of electromagnetic wave shielding mechanisms by combining the strong attenuation ability of the magnetic NiCo/MXene and the high electrical conductivity of carbon nanotubes (CNTs) (Figure 9). Although the electrical conductivity is lower than that of pure CNT and pure MXene films, the EMI shielding effectiveness of NiCo/MXene–CNT composite films is better than them.

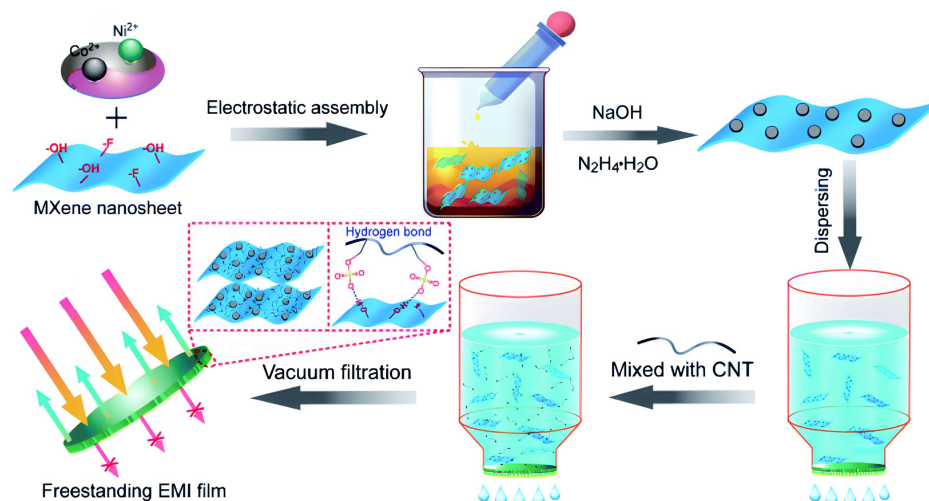


Figure 9. Schematic illustration of the preparation process of NiCo/MXene–CNT film. Reproduced from [99], with the permission of the Royal Society of Chemistry.

4.3. Other Fields

V-MXene film inherits many eminent characteristics of MXene (such as easy to intercalate, superior electrical conductivity and thermal conductivity, photothermal conversion performance and hydrophilicity), which is significantly beneficial for its application in the field of actuators. Based on the electrical conductivity and hydrophilicity of V-MXene films, our group [100] prepared a highly conductive monolayer homogeneous pure V-MXene film actuator that can be driven by moisture gradient for the first time (Figure 10), proving that single MXene is also suitable as a promising humidity actuating material, and V-MXene films can show excellent actuation ability similar to graphene oxide films. Moreover, based on the high electrical conductivity, hydrophilicity and photothermal conversion ability of V-MXene films, Cai et al. [101] prepared a V-MXene-based film actuator that can respond to moisture, light and electricity at the same time.

Based on the photothermal conversion characteristics of V-MXene films, Li et al. [102] investigated the potential of V-MXene films in the field of seawater desalination. In the presence of an ideal heat barrier, the light to water evaporation efficiency of the self-floating V-MXene film can reach 84%. V-MXene films have regular interlayer transport channels and a large number of surface functional groups, which are helpful to sieve and separate various gas molecules. The two-dimensional lamellar structure of V-MXene film allows hydrogen to pass freely and gases with large sizes will be blocked. Therefore, it shows outstanding gas separation ability. H₂ permeability is greater than 2200 Barrer, and the selectivity of H₂/CO₂ is more than 160 [103]. On account of the low mid infrared emissivity of MXene (Figure 11a), V-MXene film can also be used in the field of infrared stealth. Li et al. [104] prepared an ultra-thin V-MXene film with a thickness as low as 1 μm, which can reduce the radiation temperature of high-temperature objects above 500 °C by more than 300 °C (Figure 11b), superior to the reported thermal camouflage materials/coating materials. V-MXene based films can also be used for catalysis. Ma et al. [105] fabricated a composite film composed of two-dimensional graphitic carbon nitride and MXene, and applied it to catalyze the oxygen-evolution reaction in an alkaline aqueous system. The composite film shows superior catalytic activity and stability, which is comparable to the

state-of-the-art precious/transition-metal catalysts. Additionally, V-MXene film can also be applied to sensor [106], water purification [74], antibacterial [107], aroma molecules adsorption and release [108], fire prevention [109] and other fields.

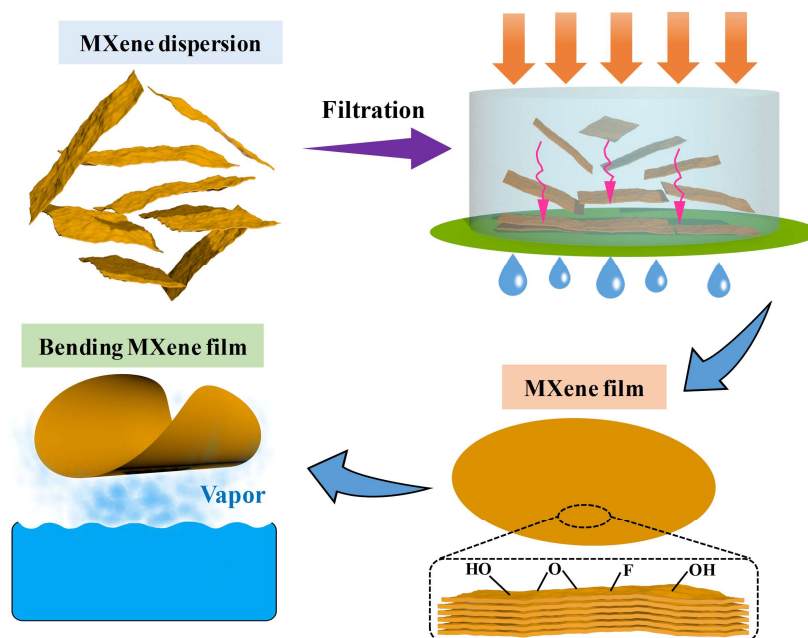


Figure 10. Schematic illustration of the preparation process of highly conductive monolayer homogeneous pure V-MXene film actuator. Reproduced from [100], with the permission of Wiley-VCH.

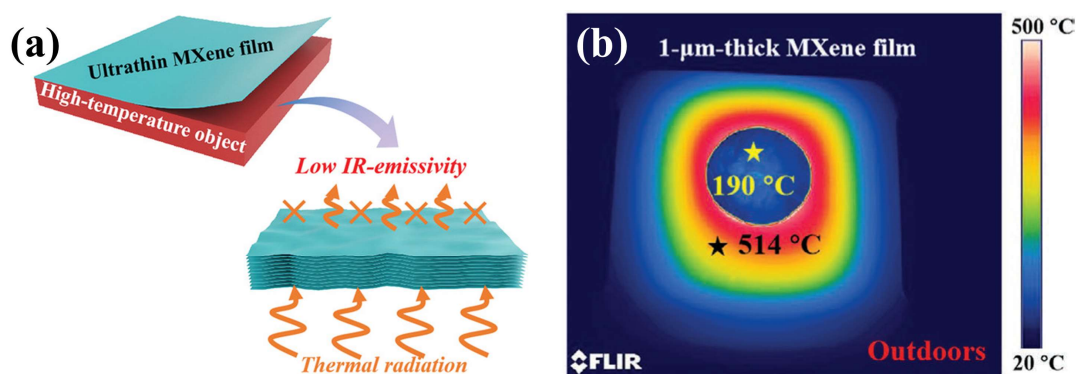


Figure 11. (a) Schematic illustration of the thermal camouflage mechanism of the V-MXene film. (b) IR thermal image of V-MXene film (thickness: 1 μm) on a hot object (514 $^{\circ}\text{C}$). Reproduced from [104], with the permission of Wiley-VCH.

5. Summary and Outlook

This paper summarized the research progress of V-MXene films, introduced the synthesis of MXene nanosheets and the preparation process of V-MXene films, discussed the properties of V-MXene films, and reviewed the application potential of V-MXene films in the fields of energy storage, EMI shielding, actuators and so on. Although a series of significant progress has been made on V-MXene films, some existing problems also make it a certain distance from the practical application.

First of all, at present, MXene is mainly prepared by HF direct etching or in situ HF etching of its precursor; accordingly, it is potentially dangerous to the human body, and will produce a large amount of waste acid and waste liquid, which is disadvanta-

geous to environmental protection. It is still difficult to prepare MXene on a large scale. Therefore, it is still an urgent problem to develop a low-cost, green and efficient MXene preparation process.

The structural defects, surface groups and size of MXene nanosheets have a significant impact on various properties of V-MXene films, such as electrical conductivity, mechanical properties and wettability. Investigating the mapping relationship between the preparation process of MXene nanosheets, the structure of nanosheets and the properties of V-MXene films, establishing a theoretical model among the three, and then optimizing the MXene preparation process suitable for the application of V-MXene films in specific fields are research directions that need to be mainly emphasized in the future.

Significant progress has been made in the previous research on overcoming the dense structure of V-MXene films. However, the development of simpler technologies for preparing V-MXene films with internal mass transfer channels is still the important direction of future research, which is of great significance for the application of electrochemical energy storage, seawater desalination, osmotic power generation and other fields. At the same time, precise control of the internal pore size and distribution of V-MXene films is also a research emphasis in the future. Preparing ultra-thin and highly transparent V-MXene films and highly oriented and dense V-MXene films (compared with MXene films prepared by blade-coating, drop-casting under the same conditions) are also the focus of future research.

In addition, the previous research has reduced the preparation time of V-MXene film [47] and overcame the problem that the size of V-MXene film cannot increase [84]. However, the two technologies are still difficult to be compatible (the V-MXene film prepared by electrolyte-induced flocculation combined with vacuum-assisted filtration will lose the weldability). In the future, we should look for a suitable reagent (which can not only induce the gel of MXene dispersion, accelerate the preparation of V-MXene film, but also can be completely removed in the subsequent treatment without affecting the weldability of V-MXene film), to realize the expansion of V-MXene film size and the construction of complex MXene structure on the premise that V-MXene film can be prepared on a large scale, and further promote the real application and commercialization of V-MXene film.

Author Contributions: J.W.: Conceptualization, investigation, writing—original draft. J.H., D.K., K.C. and M.S.: Investigation. W.H.: Conceptualization, investigation, supervision, writing—review and editing. All authors have read and agreed to the published version of the manuscript.

Funding: This work was financially supported by the National Science Basic Research Plan in the Shaanxi Province of China (2022JQ-521 and 2022JQ-012), Key Research and Development Program of Shaanxi Province (2021SF-296) and Northwest Institute for Nonferrous Metal Research (YK1904, YK2020-7, YK2107 and YK2114).

Institutional Review Board Statement: Not applicable.

Informed Consent Statement: Not applicable.

Data Availability Statement: Not applicable.

Conflicts of Interest: The authors declare no conflict of interest.

References

1. Rasheed, P.A.; Pandey, R.P.; Banat, F.; Hasan, S.W. Recent Advances in Niobium MXenes: Synthesis, Properties, and Emerging Applications. *Matter* **2022**, *5*, 546–572. [[CrossRef](#)]
2. VahidMohammadi, A.; Rosen, J.; Gogotsi, Y. The World of Two-Dimensional Carbides and Nitrides (MXenes). *Science* **2021**, *372*, eabf1581. [[CrossRef](#)]
3. Mathis, T.S.; Maleski, K.; Goad, A.; Sarycheva, A.; Anayee, M.; Foucher, A.C.; Hantanasirisakul, K.; Shuck, C.E.; Stach, E.A.; Gogotsi, Y. Modified MAX Phase Synthesis for Environmentally Stable and Highly Conductive Ti_3C_2 MXene. *ACS Nano* **2021**, *15*, 6420–6429. [[CrossRef](#)]
4. Lipatov, A.; Goad, A.; Loes, M.J.; Vorobeva, N.S.; Abourahma, J.; Gogotsi, Y.; Sinitskii, A. High Electrical Conductivity and Breakdown Current Density of Individual Monolayer $Ti_3C_2T_x$ MXene Flakes. *Matter* **2021**, *4*, 1413–1427. [[CrossRef](#)]
5. Ghidui, M.; Lukatskaya, M.R.; Zhao, M.-Q.; Gogotsi, Y.; Barsoum, M.W. Conductive Two-Dimensional Titanium Carbide ‘Clay’ with High Volumetric Capacitance. *Nature* **2014**, *516*, 78–81. [[CrossRef](#)] [[PubMed](#)]

6. Chen, J.; Ding, Y.; Yan, D.; Huang, J.; Peng, S. Synthesis of MXene and Its Application for Zinc-Ion Storage. *SusMat* **2022**, *2*, 293–318. [[CrossRef](#)]
7. Li, N.; Peng, J.; Ong, W.-J.; Ma, T.; Arramel; Zhang, P.; Jiang, J.; Yuan, X.; Zhang, C. MXenes: An Emerging Platform for Wearable Electronics and Looking Beyond. *Matter* **2021**, *4*, 377–407. [[CrossRef](#)]
8. Abdolhosseinzadeh, S.; Jiang, X.; Zhang, H.; Qiu, J.; Zhang, C. Perspectives on Solution Processing of Two-Dimensional MXenes. *Mater. Today* **2021**, *48*, 214–240. [[CrossRef](#)]
9. Levitt, A.; Zhang, J.; Dion, G.; Gogotsi, Y.; Razal, J.M. MXene-Based Fibers, Yarns, and Fabrics for Wearable Energy Storage Devices. *Adv. Funct. Mater.* **2020**, *30*, 2000739. [[CrossRef](#)]
10. Zhang, J.; Kong, N.; Uzun, S.; Levitt, A.; Seyedin, S.; Lynch, P.A.; Qin, S.; Han, M.; Yang, W.; Liu, J.; et al. Scalable Manufacturing of Free-Standing, Strong $\text{Ti}_3\text{C}_2\text{T}_x$ MXene Films with Outstanding Conductivity. *Adv. Mater.* **2020**, *32*, 2001093. [[CrossRef](#)]
11. Adomavičiūtė-Grabusovė, S.; Ramanavičius, S.; Popov, A.; Šablinskas, V.; Gogotsi, O.; Ramanavičius, A. Selective Enhancement of SERS Spectral Bands of Salicylic Acid Adsorbate on 2D $\text{Ti}_3\text{C}_2\text{T}_x$ -Based MXene Film. *Chemosensors* **2021**, *9*, 223. [[CrossRef](#)]
12. Ramanavičius, S.; Ramanavičius, A. Progress and Insights in the Application of MXenes as New 2D Nano-Materials Suitable for Biosensors and Biofuel Cell Design. *Int. J. Mol. Sci.* **2020**, *21*, 9224. [[CrossRef](#)] [[PubMed](#)]
13. Wang, W.; Cai, T.; Cheng, Z.; Yang, Y.; Wang, J.; Tang, J.; Tang, L.; Feng, W.; Liu, Y.; Fan, Z. A Shape Programmable MXene-Based Supermolecular Nanocomposite Film. *Compos. Part A Appl. Sci. Manuf.* **2022**, *159*, 106997. [[CrossRef](#)]
14. Eom, W.; Shin, H.; Ambade, R.B.; Lee, S.H.; Lee, K.H.; Kang, D.J.; Han, T.H. Large-Scale Wet-Spinning of Highly Electroconductive MXene Fibers. *Nat. Commun.* **2020**, *11*, 2825. [[CrossRef](#)]
15. Shin, H.; Eom, W.; Lee, K.H.; Jeong, W.; Kang, D.J.; Han, T.H. Highly Electroconductive and Mechanically Strong $\text{Ti}_3\text{C}_2\text{T}_x$ MXene Fibers Using a Deformable MXene Gel. *ACS Nano* **2021**, *15*, 3320–3329. [[CrossRef](#)] [[PubMed](#)]
16. Zhang, S.; Tu, T.; Li, T.; Cai, Y.; Wang, Z.; Zhou, Y.; Wang, D.; Fang, L.; Ye, X.; Liang, B. 3D MXene/PEDOT:PSS Composite Aerogel with a Controllable Patterning Property for Highly Sensitive Wearable Physical Monitoring and Robotic Tactile Sensing. *ACS Appl. Mater. Interfaces* **2022**, *14*, 23877–23887. [[CrossRef](#)]
17. Yang, C.; Wu, X.; Xia, H.; Zhou, J.; Wu, Y.; Yang, R.; Zhou, G.; Qiu, L. 3D Printed Template-Assisted Assembly of Additive-Free $\text{Ti}_3\text{C}_2\text{T}_x$ MXene Microlattices with Customized Structures toward High Areal Capacitance. *ACS Nano* **2022**, *16*, 2699–2710. [[CrossRef](#)]
18. Zhao, M.-Q.; Xie, X.; Ren, C.E.; Makaryan, T.; Anasori, B.; Wang, G.; Gogotsi, Y. Hollow MXene Spheres and 3D Macroporous MXene Frameworks for Na-Ion Storage. *Adv. Mater.* **2017**, *29*, 1702410. [[CrossRef](#)]
19. Zhao, Q.; Zhu, Q.; Miao, J.; Zhang, P.; Wan, P.; He, L.; Xu, B. Flexible 3D Porous MXene Foam for High-Performance Lithium-Ion Batteries. *Small* **2019**, *15*, 1904293. [[CrossRef](#)]
20. Ma, H.; Li, C.; Yang, Y.; Fan, Z. 3D Porous MXene Films for Advanced Electromagnetic Interference Shielding and Capacitive Storage. *Crystals* **2022**, *12*, 780. [[CrossRef](#)]
21. Lipton, J.; Weng, G.-M.; Röhr, J.A.; Wang, H.; Taylor, A.D. Layer-by-Layer Assembly of Two-Dimensional Materials: Meticulous Control on the Nanoscale. *Matter* **2020**, *2*, 1148–1165. [[CrossRef](#)]
22. Xiong, D.; Shi, Y.; Yang, H.Y. Rational Design of MXene-Based Films for Energy Storage: Progress, Prospects. *Mater. Today* **2021**, *46*, 183–211. [[CrossRef](#)]
23. Lipton, J.; Röhr, J.A.; Dang, V.; Goad, A.; Maleski, K.; Lavini, F.; Han, M.; Tsai, E.H.R.; Weng, G.-M.; Kong, J.; et al. Scalable, Highly Conductive, and Micropatternable MXene Films for Enhanced Electromagnetic Interference Shielding. *Matter* **2020**, *3*, 546–557. [[CrossRef](#)]
24. Dillon, A.D.; Ghidoui, M.J.; Krick, A.L.; Griggs, J.; May, S.J.; Gogotsi, Y.; Barsoum, M.W.; Fafarman, A.T. Highly Conductive Optical Quality Solution-Processed Films of 2D Titanium Carbide. *Adv. Funct. Mater.* **2016**, *26*, 4162–4168. [[CrossRef](#)]
25. Hantanasirisakul, K.; Zhao, M.-Q.; Urbankowski, P.; Halim, J.; Anasori, B.; Kota, S.; Ren, C.E.; Barsoum, M.W.; Gogotsi, Y. Fabrication of $\text{Ti}_3\text{C}_2\text{T}_x$ MXene Transparent Thin Films with Tunable Optoelectronic Properties. *Adv. Electron. Mater.* **2016**, *2*, 1600050. [[CrossRef](#)]
26. Vural, M.; Pena-Francesch, A.; Bars-Pomes, J.; Jung, H.; Gudapati, H.; Hatter, C.B.; Allen, B.D.; Anasori, B.; Ozbolat, I.T.; Gogotsi, Y.; et al. Inkjet Printing of Self-Assembled 2D Titanium Carbide and Protein Electrodes for Stimuli-Responsive Electromagnetic Shielding. *Adv. Funct. Mater.* **2018**, *28*, 1801972. [[CrossRef](#)]
27. Lipton, J.; Weng, G.-M.; Alhabeab, M.; Maleski, K.; Antonio, F.; Kong, J.; Gogotsi, Y.; Taylor, A.D. Mechanically Strong and Electrically Conductive Multilayer MXene Nanocomposites. *Nanoscale* **2019**, *11*, 20295–20300. [[CrossRef](#)]
28. Sun, N.; Guan, Z.; Zhu, Q.; Anasori, B.; Gogotsi, Y.; Xu, B. Enhanced Ionic Accessibility of Flexible MXene Electrodes Produced by Natural Sedimentation. *Nano Micro Lett.* **2020**, *12*, 89. [[CrossRef](#)] [[PubMed](#)]
29. Li, J.; Yuan, X.; Lin, C.; Yang, Y.; Xu, L.; Du, X.; Xie, J.; Lin, J.; Sun, J. Achieving High Pseudocapacitance of 2D Titanium Carbide (MXene) by Cation Intercalation and Surface Modification. *Adv. Energy Mater.* **2017**, *7*, 1602725. [[CrossRef](#)]
30. Ajnsztajn, A.; Ferguson, S.; Thostenson, J.O.; Ngaboyamahina, E.; Parker, C.B.; Glass, J.T.; Stiff-Roberts, A.D. Transparent MXene-Polymer Supercapacitive Film Deposited Using RIR-MAPLE. *Crystals* **2020**, *10*, 152. [[CrossRef](#)]
31. Ling, Z.; Ren, C.E.; Zhao, M.-Q.; Yang, J.; Giammarco, J.M.; Qiu, J.; Barsoum, M.W.; Gogotsi, Y. Flexible and Conductive MXene Films and Nanocomposites with High Capacitance. *Proc. Natl. Acad. Sci. USA* **2014**, *111*, 16676. [[CrossRef](#)] [[PubMed](#)]
32. Shuck, C.E.; Sarycheva, A.; Anayee, M.; Levitt, A.; Zhu, Y.; Uzun, S.; Balitskiy, V.; Zahorodna, V.; Gogotsi, O.; Gogotsi, Y. Scalable Synthesis of $\text{Ti}_3\text{C}_2\text{T}_x$ MXene. *Adv. Eng. Mater.* **2020**, *22*, 1901241. [[CrossRef](#)]

33. Che, X.; Zhang, W.; Long, L.; Zhang, X.; Pei, D.; Li, M.; Li, C. Mildly Peeling Off and Encapsulating Large MXene Nanosheets with Rigid Biologic Fibrils for Synchronization of Solar Evaporation and Energy Harvest. *ACS Nano* **2022**, *16*, 8881–8890. [[CrossRef](#)] [[PubMed](#)]
34. Halim, J.; Lukatskaya, M.R.; Cook, K.M.; Lu, J.; Smith, C.R.; Näslund, L.-Å.; May, S.J.; Hultman, L.; Gogotsi, Y.; Eklund, P.; et al. Transparent Conductive Two-Dimensional Titanium Carbide Epitaxial Thin Films. *Chem. Mater.* **2014**, *26*, 2374–2381. [[CrossRef](#)]
35. Li, T.; Yao, L.; Liu, Q.; Gu, J.; Luo, R.; Li, J.; Yan, X.; Wang, W.; Liu, P.; Chen, B.; et al. Fluorine-Free Synthesis of High-Purity $Ti_3C_2T_x$ (T = OH, O) via Alkali Treatment. *Angew. Chem. Int. Ed.* **2018**, *57*, 6115–6119. [[CrossRef](#)]
36. Yang, S.; Zhang, P.; Wang, F.; Ricciardulli, A.G.; Lohe, M.R.; Blom, P.W.M.; Feng, X. Fluoride-Free Synthesis of Two-Dimensional Titanium Carbide (MXene) Using a Binary Aqueous System. *Angew. Chem. Int. Ed.* **2018**, *57*, 15491–15495. [[CrossRef](#)]
37. Shi, H.; Zhang, P.; Liu, Z.; Park, S.; Lohe, M.R.; Wu, Y.; Shaygan Nia, A.; Yang, S.; Feng, X. Ambient-Stable Two-Dimensional Titanium Carbide (MXene) Enabled by Iodine Etching. *Angew. Chem. Int. Ed.* **2021**, *60*, 8689–8693. [[CrossRef](#)]
38. Liang, L.; Niu, L.; Wu, T.; Zhou, D.; Xiao, Z. Fluorine-Free Fabrication of MXene via Photo-Fenton Approach for Advanced Lithium–Sulfur Batteries. *ACS Nano* **2022**, *16*, 7971–7981. [[CrossRef](#)]
39. Natu, V.; Pai, R.; Sokol, M.; Carey, M.; Kalra, V.; Barsoum, M.W. 2D $Ti_3C_2T_z$ MXene Synthesized by Water-Free Etching of Ti_3AlC_2 in Polar Organic Solvents. *Chem* **2020**, *6*, 616–630. [[CrossRef](#)]
40. Li, M.; Lu, J.; Luo, K.; Li, Y.; Chang, K.; Chen, K.; Zhou, J.; Rosen, J.; Hultman, L.; Eklund, P.; et al. Element Replacement Approach by Reaction with Lewis Acidic Molten Salts to Synthesize Nanolaminated MAX Phases and MXenes. *J. Am. Chem. Soc.* **2019**, *141*, 4730–4737. [[CrossRef](#)]
41. Li, Y.; Shao, H.; Lin, Z.; Lu, J.; Liu, L.; Duployer, B.; Persson, P.O.Å.; Eklund, P.; Hultman, L.; Li, M.; et al. A General Lewis Acidic Etching Route for Preparing MXenes with Enhanced Electrochemical Performance in Non-Aqueous Electrolyte. *Nat. Mater.* **2020**, *19*, 894–899. [[CrossRef](#)]
42. Liu, L.; Orbay, M.; Luo, S.; Duluard, S.; Shao, H.; Harmel, J.; Rozier, P.; Taberna, P.-L.; Simon, P. Exfoliation and Delamination of $Ti_3C_2T_x$ MXene Prepared via Molten Salt Etching Route. *ACS Nano* **2022**, *16*, 111–118. [[CrossRef](#)]
43. Zhang, Q.; Lai, H.; Fan, R.; Ji, P.; Fu, X.; Li, H. High Concentration of $Ti_3C_2T_x$ MXene in Organic Solvent. *ACS Nano* **2021**, *15*, 5249–5262. [[CrossRef](#)] [[PubMed](#)]
44. Alhabeab, M.; Maleski, K.; Mathis, T.S.; Sarycheva, A.; Hatter, C.B.; Uzun, S.; Levitt, A.; Gogotsi, Y. Selective Etching of Silicon from Ti_3SiC_2 (MAX) to Obtain 2D Titanium Carbide (MXene). *Angew. Chem. Int. Ed.* **2018**, *57*, 5444–5448. [[CrossRef](#)] [[PubMed](#)]
45. Ma, G.; Shao, H.; Xu, J.; Liu, Y.; Huang, Q.; Taberna, P.-L.; Simon, P.; Lin, Z. Li-Ion Storage Properties of Two-Dimensional Titanium-Carbide Synthesized via Fast One-Pot Method in Air Atmosphere. *Nat. Commun.* **2021**, *12*, 5085. [[CrossRef](#)] [[PubMed](#)]
46. Zhang, Y.-Z.; El-Demellawi, J.K.; Jiang, Q.; Ge, G.; Liang, H.; Lee, K.; Dong, X.; Alshareef, H.N. MXene Hydrogels: Fundamentals and Applications. *Chem. Soc. Rev.* **2020**, *49*, 7229–7251. [[CrossRef](#)]
47. Wang, J.; Kang, H.; Ma, H.; Liu, Y.; Xie, Z.; Wang, Y.; Fan, Z. Super-Fast Fabrication of MXene Film through a Combination of Ion Induced Gelation and Vacuum-Assisted Filtration. *Eng. Sci.* **2021**, *15*, 57–66. [[CrossRef](#)]
48. Lipatov, A.; Alhabeab, M.; Lukatskaya, M.R.; Boson, A.; Gogotsi, Y.; Sinitskii, A. Effect of Synthesis on Quality, Electronic Properties and Environmental Stability of Individual Monolayer Ti_3C_2 MXene Flakes. *Adv. Electron. Mater.* **2016**, *2*, 1600255. [[CrossRef](#)]
49. Naguib, M.; Mochalin, V.N.; Barsoum, M.W.; Gogotsi, Y. 25th Anniversary Article: MXenes: A New Family of Two-Dimensional Materials. *Adv. Mater.* **2014**, *26*, 992–1005. [[CrossRef](#)]
50. Wang, H.; Wu, Y.; Zhang, J.; Li, G.; Huang, H.; Zhang, X.; Jiang, Q. Enhancement of the Electrical Properties of MXene Ti_3C_2 Nanosheets by Post-Treatments of Alkalization and Calcination. *Mater. Lett.* **2015**, *160*, 537–540. [[CrossRef](#)]
51. Pierson, H.O. *Handbook of Carbon, Graphite, Diamonds and Fullerenes*; William Andrew Publishing: Oxford, UK, 1993.
52. Hu, T.; Zhang, H.; Wang, J.; Li, Z.; Hu, M.; Tan, J.; Hou, P.; Li, F.; Wang, X. Anisotropic Electronic Conduction in Stacked Two-Dimensional Titanium Carbide. *Sci. Rep.* **2015**, *5*, 16329. [[CrossRef](#)] [[PubMed](#)]
53. Chen, H.; Wen, Y.; Qi, Y.; Zhao, Q.; Qu, L.; Li, C. Pristine Titanium Carbide MXene Films with Environmentally Stable Conductivity and Superior Mechanical Strength. *Adv. Funct. Mater.* **2020**, *30*, 1906996. [[CrossRef](#)]
54. Iqbal, A.; Shahzad, F.; Hantanasirisakul, K.; Kim, M.-K.; Kwon, J.; Hong, J.; Kim, H.; Kim, D.; Gogotsi, Y.; Koo Chong, M. Anomalous Absorption of Electromagnetic Waves by 2D Transition Metal Carbonitride Ti_3CNT_x (MXene). *Science* **2020**, *369*, 446–450. [[CrossRef](#)] [[PubMed](#)]
55. Wan, S.; Li, X.; Chen, Y.; Liu, N.; Du, Y.; Dou, S.; Jiang, L.; Cheng, Q. High-Strength Scalable MXene Films through Bridging-Induced Densification. *Science* **2021**, *374*, 96–99. [[CrossRef](#)]
56. Borysiuk, V.N.; Mochalin, V.N.; Gogotsi, Y. Molecular Dynamic Study of the Mechanical Properties of Two-Dimensional Titanium Carbides $Ti_{n+1}C_n$ (MXenes). *Nanotechnology* **2015**, *26*, 265705. [[CrossRef](#)] [[PubMed](#)]
57. Lipatov, A.; Lu, H.; Alhabeab, M.; Anasori, B.; Gruverman, A.; Gogotsi, Y.; Sinitskii, A. Elastic Properties of 2D $Ti_3C_2T_x$ MXene Monolayers and Bilayers. *Sci. Adv.* **2018**, *4*, eaat0491. [[CrossRef](#)]
58. Luo, S.; Patole, S.; Anwer, S.; Li, B.; Delclos, T.; Gogotsi, O.; Zahorodna, V.; Balitskyi, V.; Liao, K. Tensile Behaviors of $Ti_3C_2T_x$ (MXene) Films. *Nanotechnology* **2020**, *31*, 395704. [[CrossRef](#)]
59. Li, G.; Wyatt, B.C.; Song, F.; Yu, C.; Wu, Z.; Xie, X.; Anasori, B.; Zhang, N. 2D Titanium Carbide (MXene) Based Films: Expanding the Frontier of Functional Film Materials. *Adv. Funct. Mater.* **2021**, *31*, 2105043. [[CrossRef](#)]
60. Hu, T.; Hu, M.; Li, Z.; Zhang, H.; Zhang, C.; Wang, J.; Wang, X. Interlayer Coupling in Two-Dimensional Titanium Carbide MXenes. *Phys. Chem. Chem. Phys.* **2016**, *18*, 20256–20260. [[CrossRef](#)]

61. Cao, J.; Zhou, Z.; Song, Q.; Chen, K.; Su, G.; Zhou, T.; Zheng, Z.; Lu, C.; Zhang, X. Ultrarobust $Ti_3C_2T_x$ MXene-Based Soft Actuators via Bamboo-Inspired Mesoscale Assembly of Hybrid Nanostructures. *ACS Nano* **2020**, *14*, 7055–7065. [[CrossRef](#)]
62. VahidMohammadi, A.; Moncada, J.; Chen, H.; Kayali, E.; Orangi, J.; Carrero, C.A.; Beidaghi, M. Thick and Freestanding MXene/PANI Pseudocapacitive Electrodes with Ultrahigh Specific Capacitance. *J. Mater. Chem. A* **2018**, *6*, 22123–22133. [[CrossRef](#)]
63. Cao, W.-T.; Chen, F.-F.; Zhu, Y.-J.; Zhang, Y.-G.; Jiang, Y.-Y.; Ma, M.-G.; Chen, F. Binary Strengthening and Toughening of MXene/Cellulose Nanofiber Composite Paper with Nacre-Inspired Structure and Superior Electromagnetic Interference Shielding Properties. *ACS Nano* **2018**, *12*, 4583–4593. [[CrossRef](#)] [[PubMed](#)]
64. Boota, M.; Anasori, B.; Voigt, C.; Zhao, M.-Q.; Barsoum, M.W.; Gogotsi, Y. Pseudocapacitive Electrodes Produced by Oxidant-Free Polymerization of Pyrrole between the Layers of 2D Titanium Carbide (MXene). *Adv. Mater.* **2016**, *28*, 1517–1522. [[CrossRef](#)]
65. Zhou, T.; Wu, C.; Wang, Y.; Tomsia, A.P.; Li, M.; Saiz, E.; Fang, S.; Baughman, R.H.; Jiang, L.; Cheng, Q. Super-Tough MXene-Functionalized Graphene Sheets. *Nat. Commun.* **2020**, *11*, 2077. [[CrossRef](#)]
66. Xu, W.; Xu, Z.; Liang, Y.; Liu, L.; Weng, W. Enhanced Tensile and Electrochemical Performance of MXene/CNT Hierarchical Film. *Nanotechnology* **2021**, *32*, 355706. [[CrossRef](#)]
67. Wan, S.; Li, X.; Wang, Y.; Chen, Y.; Xie, X.; Yang, R.; Tomsia, A.P.; Jiang, L.; Cheng, Q. Strong Sequentially Bridged MXene Sheets. *Proc. Natl. Acad. Sci. USA* **2020**, *117*, 27154. [[CrossRef](#)] [[PubMed](#)]
68. Zhao, X.; Vashisth, A.; Prehn, E.; Sun, W.; Shah, S.A.; Habib, T.; Chen, Y.; Tan, Z.; Lutkenhaus, J.L.; Radovic, M.; et al. Antioxidants Unlock Shelf-Stable $Ti_3C_2T_x$ (MXene) Nanosheet Dispersions. *Matter* **2019**, *1*, 513–526. [[CrossRef](#)]
69. Anasori, B.; Gogotsi, Y. *2D Metal Carbides and Nitrides (MXenes) Structure, Properties and Applications Structure, Properties and Applications*; Springer: Gewerbestrasse, Switzerland, 2019.
70. Habib, T.; Zhao, X.; Shah, S.A.; Chen, Y.; Sun, W.; An, H.; Lutkenhaus, J.L.; Radovic, M.; Green, M.J. Oxidation Stability of $Ti_3C_2T_x$ MXene Nanosheets in Solvents and Composite Films. *NPJ 2D Mater. Appl.* **2019**, *3*, 8. [[CrossRef](#)]
71. Yang, W.; Liu, J.-J.; Wang, L.-L.; Wang, W.; Yuen, A.C.Y.; Peng, S.; Yu, B.; Lu, H.-D.; Yeoh, G.H.; Wang, C.-H. Multifunctional MXene/Natural Rubber Composite Films with Exceptional Flexibility and Durability. *Compos. Part B Eng.* **2020**, *188*, 107875. [[CrossRef](#)]
72. Jia, G.; Zheng, A.; Wang, X.; Zhang, L.; Li, L.; Li, C.; Zhang, Y.; Cao, L. Flexible, Biocompatible and Highly Conductive MXene-Graphene Oxide Film for Smart Actuator and Humidity Sensor. *Sens. Actuators B Chem.* **2021**, *346*, 130507. [[CrossRef](#)]
73. Wang, J.; Chen, P.; Shi, B.; Guo, W.; Jaroniec, M.; Qiao, S.-Z. A Regularly Channeled Lamellar Membrane for Unparalleled Water and Organics Permeation. *Angew. Chem. Int. Ed.* **2018**, *57*, 6814–6818. [[CrossRef](#)]
74. Xie, X.; Chen, C.; Zhang, N.; Tang, Z.-R.; Jiang, J.; Xu, Y.-J. Microstructure and Surface Control of MXene Films for Water Purification. *Nat. Sustain.* **2019**, *2*, 856–862. [[CrossRef](#)]
75. Bian, R.; Xiang, S.; Cai, D. Fast Treatment of MXene Films with Isocyanate to Give Enhanced Stability. *ChemNanoMat* **2020**, *6*, 64–67. [[CrossRef](#)]
76. Zhang, B.; Gu, Q.; Wang, C.; Gao, Q.; Guo, J.; Wong, P.W.; Liu, C.T.; An, A.K. Self-Assembled Hydrophobic/Hydrophilic Porphyrin- $Ti_3C_2T_x$ MXene Janus Membrane for Dual-Functional Enabled Photothermal Desalination. *ACS Appl. Mater. Interfaces* **2021**, *13*, 3762–3770. [[CrossRef](#)] [[PubMed](#)]
77. Yang, J.; Wang, C.; Liu, L.; Zhang, H.; Ma, J. Water-Tolerant MXene Epidermal Sensors with High Sensitivity and Reliability for Healthcare Monitoring. *ACS Appl. Mater. Interfaces* **2022**, *14*, 21253–21262. [[CrossRef](#)]
78. Zhao, J.; Yang, Y.; Yang, C.; Tian, Y.; Han, Y.; Liu, J.; Yin, X.; Que, W. A Hydrophobic Surface Enabled Salt-Blocking 2D Ti_3C_2 MXene Membrane for Efficient and Stable Solar Desalination. *J. Mater. Chem. A* **2018**, *6*, 16196–16204. [[CrossRef](#)]
79. Fan, Z.; Wang, Y.; Xie, Z.; Xu, X.; Yuan, Y.; Cheng, Z.; Liu, Y. A Nanoporous MXene Film Enables Flexible Supercapacitors with High Energy Storage. *Nanoscale* **2018**, *10*, 9642–9652. [[CrossRef](#)]
80. Zhou, H.; Wang, F.; Wang, Y.; Li, C.; Shi, C.; Liu, Y.; Ling, Z. Study on Contact Angles and Surface Energy of MXene Films. *RSC Adv.* **2021**, *11*, 5512–5520. [[CrossRef](#)]
81. Liu, J.; Zhang, H.-B.; Sun, R.; Liu, Y.; Liu, Z.; Zhou, A.; Yu, Z.-Z. Hydrophobic, Flexible, and Lightweight MXene Foams for High-Performance Electromagnetic-Interference Shielding. *Adv. Mater.* **2017**, *29*, 1702367. [[CrossRef](#)]
82. Yin, L.; Kang, H.; Ma, H.; Wang, J.; Liu, Y.; Xie, Z.; Wang, Y.; Fan, Z. Sunshine Foaming of Compact $Ti_3C_2T_x$ MXene Film for Highly Efficient Electromagnetic Interference Shielding and Energy Storage. *Carbon* **2021**, *182*, 124–133. [[CrossRef](#)]
83. Ren, C.E.; Zhao, M.-Q.; Makaryan, T.; Halim, J.; Boota, M.; Kota, S.; Anasori, B.; Barsoum, M.W.; Gogotsi, Y. Porous Two-Dimensional Transition Metal Carbide (MXene) Flakes for High-Performance Li-Ion Storage. *ChemElectroChem* **2016**, *3*, 689–693. [[CrossRef](#)]
84. Wang, J.; Liu, Y.; Yang, Y.; Wang, J.; Kang, H.; Yang, H.; Zhang, D.; Cheng, Z.; Xie, Z.; Tan, H.; et al. A Weldable MXene Film Assisted by Water. *Matter* **2022**, *5*, 1042–1055. [[CrossRef](#)]
85. Xiong, D.; Li, X.; Bai, Z.; Lu, S. Recent Advances in Layered $Ti_3C_2T_x$ MXene for Electrochemical Energy Storage. *Small* **2018**, *14*, 1703419. [[CrossRef](#)] [[PubMed](#)]
86. Zhao, M.-Q.; Ren, C.E.; Ling, Z.; Lukatskaya, M.R.; Zhang, C.; Van Aken, K.L.; Barsoum, M.W.; Gogotsi, Y. Flexible MXene/Carbon Nanotube Composite Paper with High Volumetric Capacitance. *Adv. Mater.* **2015**, *27*, 339–345. [[CrossRef](#)] [[PubMed](#)]

87. Yang, C.; Tang, Y.; Tian, Y.; Luo, Y.; Faraz Ud Din, M.; Yin, X.; Que, W. Flexible Nitrogen-Doped 2D Titanium Carbides (MXene) Films Constructed by an Ex Situ Solvothermal Method with Extraordinary Volumetric Capacitance. *Adv. Energy Mater.* **2018**, *8*, 1802087. [[CrossRef](#)]
88. Zhu, Y.; Rajouâ, K.; Le Vot, S.; Fontaine, O.; Simon, P.; Favier, F. Modifications of MXene Layers for Supercapacitors. *Nano Energy* **2020**, *73*, 104734. [[CrossRef](#)]
89. Zhao, K.; Wang, H.; Zhu, C.; Lin, S.; Xu, Z.; Zhang, X. Free-Standing MXene Film Modified by Amorphous FeOOH Quantum Dots for High-Performance Asymmetric Supercapacitor. *Electrochim. Acta* **2019**, *308*, 1–8. [[CrossRef](#)]
90. Ma, R.; Zhang, X.; Zhuo, J.; Cao, L.; Song, Y.; Yin, Y.; Wang, X.; Yang, G.; Yi, F. Self-Supporting, Binder-Free, and Flexible $\text{Ti}_3\text{C}_2\text{T}_x$ MXene-Based Supercapacitor Electrode with Improved Electrochemical Performance. *ACS Nano* **2022**, *16*, 9713–9727. [[CrossRef](#)]
91. Ma, Z.; Zhou, X.; Deng, W.; Lei, D.; Liu, Z. 3D Porous MXene (Ti_3C_2)/Reduced Graphene Oxide Hybrid Films for Advanced Lithium Storage. *ACS Appl. Mater. Interfaces* **2018**, *10*, 3634–3643. [[CrossRef](#)]
92. Sun, N.; Zhu, Q.; Anasori, B.; Zhang, P.; Liu, H.; Gogotsi, Y.; Xu, B. MXene-Bonded Flexible Hard Carbon Film as Anode for Stable Na/K-Ion Storage. *Adv. Funct. Mater.* **2019**, *29*, 1906282. [[CrossRef](#)]
93. Li, G.; Lian, S.; Song, F.; Chen, S.; Wu, Z.; Xie, X.; Zhang, N. Surface Chemistry and Mesopore Dual Regulation by Sulfur-Promised High Volumetric Capacity of $\text{Ti}_3\text{C}_2\text{T}_x$ Films for Sodium-Ion Storage. *Small* **2021**, *17*, 2103626. [[CrossRef](#)] [[PubMed](#)]
94. Chen, C.; Boota, M.; Xie, X.; Zhao, M.; Anasori, B.; Ren, C.E.; Miao, L.; Jiang, J.; Gogotsi, Y. Charge Transfer Induced Polymerization of EDOT Confined between 2D Titanium Carbide Layers. *J. Mater. Chem. A* **2017**, *5*, 5260–5265. [[CrossRef](#)]
95. Shahzad, F.; Alhabeab, M.; Hatter, C.B.; Anasori, B.; Man Hong, S.; Koo, C.M.; Gogotsi, Y. Electromagnetic Interference Shielding with 2D Transition Metal Carbides (MXenes). *Science* **2016**, *353*, 1137. [[CrossRef](#)]
96. Liu, Z.; Zhang, Y.; Zhang, H.-B.; Dai, Y.; Liu, J.; Li, X.; Yu, Z.-Z. Electrically Conductive Aluminum Ion-Reinforced MXene Films for Efficient Electromagnetic Interference Shielding. *J. Mater. Chem. C* **2020**, *8*, 1673–1678. [[CrossRef](#)]
97. Luo, J.-Q.; Zhao, S.; Zhang, H.-B.; Deng, Z.; Li, L.; Yu, Z.-Z. Flexible, Stretchable and Electrically Conductive MXene/Natural Rubber Nanocomposite Films for Efficient Electromagnetic Interference Shielding. *Compos. Sci. Technol.* **2019**, *182*, 107754. [[CrossRef](#)]
98. Zhou, B.; Zhang, Z.; Li, Y.; Han, G.; Feng, Y.; Wang, B.; Zhang, D.; Ma, J.; Liu, C. Flexible, Robust, and Multifunctional Electromagnetic Interference Shielding Film with Alternating Cellulose Nanofiber and MXene Layers. *ACS Appl. Mater. Interfaces* **2020**, *12*, 4895–4905. [[CrossRef](#)]
99. Liang, L.; Yao, C.; Yan, X.; Feng, Y.; Hao, X.; Zhou, B.; Wang, Y.; Ma, J.; Liu, C.; Shen, C. High-Efficiency Electromagnetic Interference Shielding Capability of Magnetic $\text{Ti}_3\text{C}_2\text{T}_x$ MXene/CNT Composite Film. *J. Mater. Chem. A* **2021**, *9*, 24560–24570. [[CrossRef](#)]
100. Wang, J.; Liu, Y.; Cheng, Z.; Xie, Z.; Yin, L.; Wang, W.; Song, Y.; Zhang, H.; Wang, Y.; Fan, Z. Highly Conductive MXene Film Actuator Based on Moisture Gradients. *Angew. Chem. Int. Ed.* **2020**, *59*, 14029–14033. [[CrossRef](#)]
101. Cai, G.; Ciou, J.-H.; Liu, Y.; Jiang, Y.; Lee, P.S. Leaf-Inspired Multiresponsive MXene-Based Actuator for Programmable Smart Devices. *Sci. Adv.* **2019**, *5*, eaaw7956. [[CrossRef](#)]
102. Li, R.; Zhang, L.; Shi, L.; Wang, P. MXene Ti_3C_2 : An Effective 2D Light-to-Heat Conversion Material. *ACS Nano* **2017**, *11*, 3752–3759. [[CrossRef](#)]
103. Ding, L.; Wei, Y.; Li, L.; Zhang, T.; Wang, H.; Xue, J.; Ding, L.-X.; Wang, S.; Caro, J.; Gogotsi, Y. MXene Molecular Sieving Membranes for Highly Efficient Gas Separation. *Nat. Commun.* **2018**, *9*, 155. [[CrossRef](#)]
104. Li, L.; Shi, M.; Liu, X.; Jin, X.; Cao, Y.; Yang, Y.; Wang, W.; Wang, J. Ultrathin Titanium Carbide (MXene) Films for High-Temperature Thermal Camouflage. *Adv. Funct. Mater.* **2021**, *31*, 2101381. [[CrossRef](#)]
105. Ma, T.Y.; Cao, J.L.; Jaroniec, M.; Qiao, S.Z. Interacting Carbon Nitride and Titanium Carbide Nanosheets for High-Performance Oxygen Evolution. *Angew. Chem. Int. Ed.* **2016**, *55*, 1138–1142. [[CrossRef](#)] [[PubMed](#)]
106. Su, T.; Liu, N.; Lei, D.; Wang, L.; Ren, Z.; Zhang, Q.; Su, J.; Zhang, Z.; Gao, Y. Flexible MXene/Bacterial Cellulose Film Sound Detector Based on Piezoresistive Sensing Mechanism. *ACS Nano* **2022**, *16*, 8461–8471. [[CrossRef](#)] [[PubMed](#)]
107. Rasool, K.; Mahmoud, K.A.; Johnson, D.J.; Helal, M.; Berdiyrov, G.R.; Gogotsi, Y. Efficient Antibacterial Membrane Based on Two-Dimensional $\text{Ti}_3\text{C}_2\text{T}_x$ (MXene) Nanosheets. *Sci. Rep.* **2017**, *7*, 1598. [[CrossRef](#)] [[PubMed](#)]
108. Ciou, J.-H.; Li, S.; Lee, P.S. Ti_3C_2 MXene Paper for the Effective Adsorption and Controllable Release of Aroma Molecules. *Small* **2019**, *15*, 1903281. [[CrossRef](#)]
109. Zhang, Y.; Cheng, W.; Tian, W.; Lu, J.; Song, L.; Liew, K.M.; Wang, B.; Hu, Y. Nacre-Inspired Tunable Electromagnetic Interference Shielding Sandwich Films with Superior Mechanical and Fire-Resistant Protective Performance. *ACS Appl. Mater. Interfaces* **2020**, *12*, 6371–6382. [[CrossRef](#)]